Inorg. Chem. **2002**, *41*, 455–461

Growth of Sb_2E_3 (E = S, Se) Polygonal Tubular Crystals via a Novel Solvent-Relief-Self-Seeding Process

Xiuwen Zheng,[†] Yi Xie,*[,†] Liying Zhu,[†] Xuchuan Jiang,[†] Yunbo Jia,[†] Wenhai Song,[‡] and Yuping Sun[‡]

Structure Research Laboratory and Laboratory of NanoChemistry and NanoMaterials, University of Science and Technology of China, Hefei, Anhui 230026, P.R. China, and Institute of Solid State Physics, Chinese Academy of Science, Hefei, Anhui 230031, P.R. China

Received July 5, 2001

A novel solvent-relief-self-seeding (SRSS) process was applied to grow bulk polygonal tubular single crystals of Sb_2E_3 (E = S, Se), using $SbCl_3$ and chalcogen elements E (E = S, Se) as the raw materials at 180 °C for 7 days in ethanol solution. The products were characterized by various techniques, including X-ray powder diffraction (XRD), scanning electronic microscope (SEM), transmission electronic microscope (TEM), electronic diffraction (ED), and X-ray photoelectron spectra (XPS). The calculated electrical resistivities of the tubular single crystals in the range 20–320 K were of the order of 10^5–10^6 Ω cm for Sb_2S_3 and 10^3–10^4 Ω cm for Sb_2Se_3, respectively. The studies of the optical properties revealed that the materials formed had a band gap of 1.72 eV for Sb_2S_3 and 1.82 eV for Sb_2Se_3, respectively. The optimal reaction conditions for the growth of bulk tubular single crystals were that the temperature was not lower than 180 °C and the reaction time was not shorter than 7 days. The possible growth mechanism of tubular crystals was also discussed.

Introduction

In recent years, one of the important goals of material chemistry has been to develop ways of tailoring the materials with open structure on a large three-dimensional (3D) mesoscale (milimeter to centimeter scale).[1−5] Though some tubular objects in the mesoscale are too large to exhibit such size-dependent properties, they have attracted special attention because of their special well-defined structure and their inherent mechanical strength,[6] their unusual electronic transport properties,[7] and their ability to act as containers or capsules[8] to provide more inert platforms for host−guest chemistry.[9] Therefore, tubular structure materials have been found to be important in potential applications in the syntheses of designed catalysts, phonic band gap materials, and chemical separations media and as selective sorbets.[10] A wide spectrum of materials with submicrometer dimensions and tubular structure have been processed, including inorganic materials (carbon, vanadium oxide, MoS_2, and WS_2)[11] and organic materials (biomolecules, polymer).[12] As is well-known, compounds possessing graphite-analogue layered structures should be able to form tubular or fullerene-type structures,[13] such as layered semiconductor compounds MQ_2 (M = W, Mo; Q = S, Se) and BN have been

* To whom correspondence should be addressed. E-mail: yxie@ustc.edu.cn.
† University of Science and Technology of China.
‡ Chinese Academy of Science.

(1) Breen, T. L.; Tien, J.; Oliver, S. R. J.; Hadzic, T.; Whitesides, G. M. *Science* **1999**, *284*, 948.
(2) Terfort, A.; Bowden, N.; Whitesides, G. M. *Nature* **1997**, *386*, 162.
(3) Parise, J. B. *Science* **1991**, *251*, 293.
(4) Yang, Q.; Tang, K. B.; Wang, C. R.; Qian, Y. T., Yu, W. C.; Zhou, G. E.; Li, F. Q. *J. Mater. Chem.* **2001**, *11*, 257.
(5) Hu, J. Q.; Deng, B.; Lu, Q. Y.; Tang, K. B.; Jiang, R. R.; Qian, Y. T.; Zhou, G. E.; Cheng, H. *Chem. Commun.* **2000**, 715.
(6) Ajayan, P. M.; Stephan, O.; Colliex, C.; Trauth, D. *Science* **1994**, *265*, 1212.
(7) Tans, S. J.; Devoret, M. H.; Dai, H.; Thess, A.; Smalley, R. E.; Geerligs, L. J.; Dekker, C. *Nature* **1997**, *386*, 474.
(8) (a) Valdes, C.; Spitz, U. P.; Toledo, L. M.; Kubik, S. W.; Rebek, J., Jr. *J. Am. Chem. Soc.* **1995**, *117*, 12733. (b) Allcock, H. R. *Acc. Chem. Res.* **1976**, *9*, 5120.
(9) (a) Ozin, G. A.; Kupernan, A.; Stein, A. *Angew. Chem., Int. Ed. Engl.* **1989**, *28*, 359. (b) Stucky, G. D.; Mac, D. J. E. *Science* **1990**, *247*, 669.
(10) (a) Ozin, G. A. *Adv. Mater.* **1992**, *4*, 612. (b) Mann, S. J. *Chem. Mater.* **1997**, *9*, 2300. (c) Yaghi, O. M.; Li, H.; Davis, C.; Richardson, D.; Groy, T. *Acc. Chem. Res.* **1998**, *31*, 474.
(11) (a) Iijima, S. *Nature* **1991**, *354*, 56. (b) Muhr, H. J.; Krumeich, F.; Schonholzer, U. P.; Bieri, F.; Niederberger, M.; Gauckler, L. J.; Nesper, R. *Adv. Mater.* **2000**, *12*, 231. (c) Zhu, Y. Q.; Hsu, W. K.; Grobert, N.; Chang, B. H.; Terrones, M.; Terrones, H.; Kroto, H. W.; Walton, D. R. M. *Chem. Mater.* **2000**, *12*, 1190. (d) Nath, M.; Govindaraj, A.; Rao, C. N. R. *Adv. Mater.* **2001**, *13*, 283.
(12) Bognitzki, M.; Hou, H.; Ishaque, M.; Frese, T.; Hellwig, M.; Schware, C.; Schaper, A.; Wendorff, J. H.; Greiner, A. *Adv. Mater.* **2000**, *12*, 637.
(13) (a) Tremel, W. *Angew. Chem., Int. Ed.* **1999**, *38* (15), 2175. (b) Homyonfer, M.; Mastai, Y.; Hershfinkel, M.; Volterra, V.; Hutchison, J. L.; Tenne, R. *J. Am. Chem. Soc.* **1996**, *118*, 7804. (c) Tenne, R.; Margulis, L.; Genut, M.; Hodes, G. *Nature* **1992**, *360*, 444.

10.1021/ic0107072 CCC: $22.00
Published on Web 01/08/2002

extensively investigated.[11d,14] Synthetic inorganic tubules made from lamellar solids in a manner analogous to forming multiwalled nanotubes from a material (carbon) are thermodynamically more stable than as lamellar solids,[15] and the physical tendency to reach the lowest energy level available would induce the sheets to curl up.[16] According to the previously reported studies, one can see that the most promising starting materials for the development of tubelike materials seem to be layered-structure compounds.

Group V−VI binary compounds (Sb_2S_3, Sb_2Se_3) are highly anisotropic semiconductors with a layered structure parallel to the growth direction and with orthorhombic crystal structure,[17] which is known to adopt a number of packing structures resulting in either trigonal prismatic or octahedral coordination of the metals within a layered matrix of chalcogens.[18] The compounds have attracted wide attention due to their good photovoltaic properties and high thermoelectric power (TEP), which allow potential applications to optical and thermoelectric cooling devices.[17b] Another important function of V−VI binary compounds is that they can be used as the starting materials for synthesizing other antimony chalcogenides with open-framework structures.[3,19]

Many methods have been developed to tailor tubular-structure inorganic materials, such as the self-assembly methods,[1,2] template-directed method,[20] chemical processing,[21] and sol−gel hydrothermal method.[11b,22] Up to now, the synthesis of mesoscale tubular crystals with longer and more well-defined structure is one of the main challenges facing materials scientists. Recently, development of the solvothermal method in the intermediate-temperature range 100−600 °C has been motivated by current interest in the design of solid-state chalcogenides with open-framework structure,[23] which are main compounds of the main-group elements antimony,[19] tin,[24] and germanium.[25] Our research group has successfully synthesized the hexagonal millimeter-sized tubular crystals Sb_2S_3[4], Ag_2Se,[5] and carbon nanotubes[26] by the solvothermal method. In the process of the bulk single crystal growth, the main problem encountered is the control of supersaturation of solutions, which would lead to formation of many crystal seeds. In this paper, we successfully combine the solvothermal process with the self-seeding technique and put forward a novel solvothermal solvent-relief-self-seeding (SRSS) process to grow Sb_2E_3 (E = S, Se) bulk tubular single crystals. The so-called SRSS process is similar to our previously reported solvothermal pressure relief (SPR) process,[27] which was conducted in an autoclave with a controlled relief valve. The detailed procedure for the SRSS process is that when the temperature reaches the desired value and the reaction time is sufficient, the relief valve is opened to gradually release the gas (ethanol) out of the autoclave. It is found that the SRSS route is an effective process to grow bulk single crystals. The possible growth mechanism of the tubular crystals has been carefully investigated, combining the phenomenological understanding of the morphological changes with the hexagonal crystal structure of Sb_2E_3 (E = S, Se).

Experimental Section

The Sb_2E_3 (E = S, Se) bulk single crystals were grown in a 50 mL Teflon lined autoclave from stoichiometric antimony trichloride and sulfur or selenium powders, respectively. The bulk single crystals of Sb_2S_3 were prepared as below: stoichiometric antimony trichloride (0.45 g, 2 mmol) and sulfur powders (0.1 g, 3 mmol) were successively loaded into the 50 mL Teflon lined autoclave, which was then filled with absolute ethanol up to 80 vol % of the capacity. The autoclave was maintained at 180 °C, while the gas of ethanol was slowly released out of the system by opening the relief valve during the reaction time of 7 days, and then cooled to room temperature. All of the acicular single crystals, with metallic light-gray color and high reflective luster, adhered to the inner wall of the autoclave. The products were carefully collected and washed with absolute ethanol and distilled water several times in order to remove the residues, and then dried in a vacuum at 60 °C for 4 h. In the case of the growth of acicular Sb_2Se_3 bulk single crystals, the process was similar to that of Sb_2S_3, namely, $SbCl_3$ (0.45 g, 2 mmol) reacting with selenium powders (0.24 g, 3 mmol).

The final products were characterized by various techniques. X-ray powder diffraction (XRD) was carried out on a Rigaku D/max rA X-ray diffractometer with Cu Kα radiation (λ = 1.54178 Å). The scan rate of 0.05°/s was applied to record the pattern in the 2θ range of 10−70°. The morphology and size of as-prepared products were observed by transmission electron microscope (TEM) images and scanning electronic microscopy (SEM) images, which were taken on a Hitachi model H-800 and performed on an X-650 scanning electronic microanalyzer, respectively. The electronic diffraction (ED) patterns were taken on a Hitachi model H-800 transmission electron microscope with a tungsten filament. To obtain further evidence for the purities and compositions of the as-prepared products, the X-ray photoelectron spectra (XPS) were used, which were performed on an ESCALab MKII X-ray photo-

(14) (a) Hamilton, E. J. M.; Dolan, S. E.; Mann, C. M.; Colijin, H. O.; McDonald, C. A.; Shore, S. G. *Science* **1993**, *260*, 659. (b) Remskar, M.; Skroba, Z.; Cleton, F.; Sanjines, R.; Levy, F. *Appl. Phys. Lett.* **1996**, *69*, 351. (c) Remskar, M.; Skroba, Z.; Regula, M.; Ballif, C.; Scanjines, R.; Levy, F. *Adv. Mater.* **1998**, *10*, 246.

(15) (a) Tenne, R.; Margulis, L.; Genut, M.; Hodes, G. *Nature* **1992**, *360*, 444. (b) Feldman, Y.; Wasserman, E.; Srolovits, D. J.; Tenne, R. *Science* **1995**, *267*, 222.

(16) Robertson, D. H.; Brenner, D. W.; White, C. T. *J. Phys. Chem.* **1992**, *96*, 6133.

(17) (a) Wyckoff, R. W. G. *Crystal structure*, 2nd ed.; Wiley: New York, 1964. (b) Rajpure, K. Y.; Lokhande, C. D.; Bhosale, C. H. *Mater. Res. Bull.* **1999**, *34* (7), 1079.

(18) Hulliger, F. *Structural Chemistry of Layered-Type Phase*; Reidel: Dordrecht, 1976.

(19) (a) Powell, A. V.; Boissiere, S.; Chippindale, A. M. *Chem. Mater.* **2000**, *12*, 182. (b) Sheldrick, W. S.; Hausler, H. J. *Z. Anorg. Allg. Chem.* **1988**, *557*, 98. (c) Volk, K.; Schafer, H. *Z. Naturforsh. B* **1979**, *34*, 172.

(20) (a) Lakshmi, B. B.; Patrissi, C. J.; Martin, C. R. *Chem. Mater.* **1997**, *9*, 2544. (b) Hoyer, P. *Langmuir* **1996**, *12*, 1411. (c) Zelenski, C. M.; Dorhout, P. K. *J. Am. Chem. Soc.* **1998**, *120*, 734. (d) Bognitzki, M.; Hou, H.; Ishaque, M.; Frese, T.; Hellwing, M.; Schware, C.; Schaper A.; Wendorff, J. H.; Greiner, A. *Adv. Mater.* **2000**, *12*, 637.

(21) Kasuga, T.; Hiramatsu, M.; Hoson, A.; Sekino, T.; Niihara, K. *Adv. Mater.* **1999**, *11*, 1307.

(22) Krumeich, F.; Muhr, H.-J.; Niederberger, M.; Bieri, F.; Schnyder, B.; Nesper, R. *J. Am. Chem. Soc.* **1999**, *121*, 8324.

(23) Sheldrick, W. S.; Wachhold, M. *Angew. Chem., Int. Ed. Engl.* **1997**, *36*, 206.

(24) Sheldrick, W. S.; Schaaf, B. *Z. Anorg. Allg. Chem.* **1994**, *620*, 1041.

(25) Sheldrick, W. S.; Schaaf, B. *Z. Naturforsch. B* **1995**, *50*, 1469.

(26) Jiang, Y.; Wu, Y.; Zhang, S. Y.; Xu, C. Y.; Yu, W. C.; Xie, Y.; Qian, Y. T. *J. Am. Chem. Soc.* **2000**, *122*, 12383.

(27) Yu, S. H.; Han, Z. H.; Yan, J.; Zhao, H. Q.; Yang, R. Y.; Xie, Y.; Qian, Y. T.; Zhang, Y. H. *Chem. Mater.* **1999**, *11*, 192.

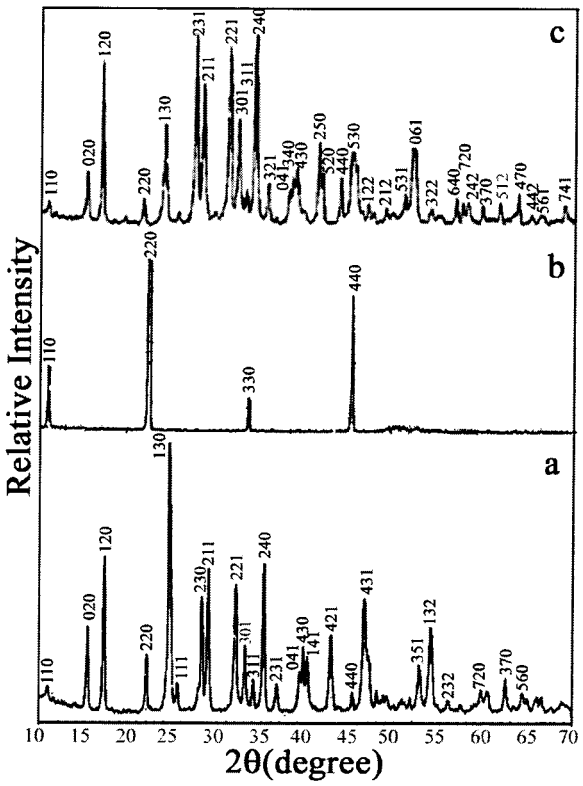

Figure 1. XRD patterns of (a) Sb_2S_3 powders, (b) Sb_2S_3 bulk single crystals, and (c) Sb_2Se_3 powders.

electron spectrometer, using a Mg Kα radiation as the exciting source. The studies of optical properties were carried out using a UV−visible recording spectrophotometer (UV-240) in the wavelength range 500−800 nm. To study the electrical characteristics of the single crystals, dark conductivity measurements were carried out on a Keithley 182 sensitive digital voltmeter and a Keithley 2400 sourcemeter, using a two-point probe method in the temperature range 20−320 K. Silver paste was applied to provide ohmic contact with the single crystals.

Results and Discussion

The XRD patterns of the polycrystalline powders ground from the acicular single crystals are shown in Figure 1, parts a (Sb_2S_3) and c (Sb_2Se_3), respectively. All the reflection peaks can be indexed to the corresponding orthorhombic pure phases with cell parameters $a = 11.189$ Å, $b = 11.291$ Å, and $c = 3.833$ Å for Sb_2S_3 as well as $a = 11.633$ Å, $b = 11.780$ Å, and $c = 3.985$ Å for Sb_2Se_3, respectively, which are very close to the data reported in the literature.[28] The XRD pattern (Figure 1b) of acicular bulk single crystals Sb_2S_3 only exhibits four peaks at 11.1°, 22.3°, 33.8°, and 45.6°, which can be assigned to the orthorhombic 110, 220, 330, and 440 planes for Sb_2S_3. Moreover, other relatively strong reflection peaks in polycrystalline powder diffraction are absent in this pattern. The above results show that the (110) plane of the orthorhombic Sb_2S_3 single crystals parallels the shaft of the acicular single crystals.

The SEM images of the as-prepared products are shown in Figure 2. Figure 2a (Sb_2S_3) and Figure 2b (Sb_2Se_3) display the randomly distributed and fairly uniform diameter tubular crystals under low magnification, respectively. Careful examinations under high magnification show that the tubular crystals exhibit a polygonal cross section for Sb_2S_3 (Figure 2c,d) and a tetragonal cross section for Sb_2Se_3 (Figure 2e,f) rather than a circular cross section. Panels c and e of Figure 2 illustrate the typical, straight hollow-core tubular crystals. Typically, this structure is 10−15 mm in length, 50−60 μm in width, and 5−10 μm in thickness for Sb_2S_3, and 5−10 mm in length, 10−20 μm in width, and 5−10 μm in thickness for Sb_2Se_3, respectively. According to Figure 2, one can see that the structure of Sb_2Se_3 is similar to that of Sb_2S_3 and the tubes are of high quality in that they are very straight and relatively long. The ED patterns of the as-prepared products are shown in Figure 2g (Sb_2S_3) and Figure 2h (Sb_2Se_3), which indicate that the Sb_2E_3 (E = S, Se) are single crystals.

The XPS spectra were carried out to identify the surface compositions of as-prepared products. No obvious impurities could be detected in the samples, indicating that the level of impurities is lower than the resolution limit of XPS (1 atm %). The typical high-resolution spectra of Sb_2E_3 (E = S, Se) are shown in Figure 3. The binding energy of Sb 4d is taken for characterization in that the position of binding energy Sb 3d is superposed with that of O 2p binding energy. The binding energy values are 34.00 eV for Sb 4d and 161.90 eV for S 2p in Sb_2S_3 (Figure 3a) and 34.20 eV for Sb 4d and 54.45 eV for Se 3d in Sb_2Se_3 (Figure 3b), respectively. All of the observed binding energy values for Sb 4d and S 2p or Se 3d coincide with the reported data.[29] Quantification of the XPS peaks gives the molar ratio of the products as 0.802:1.000 for Sb:S, and 0.654:1.000 for Sb:Se, respectively, which are nearly consistent with the given formula for the as-prepared products within the experimental errors. The spectrum (167.30 eV, Figure 3a, arrowed) indicates that a little sulfur is oxidized into S^{IV} (167.40 eV) on the surface of Sb_2S_3, which leads to the increase of the surface molar ratio of Sb to S.

The optical properties of the as-prepared bulk single crystals can be determined by the diffuse reflectance spectra, which provide a simple and effective method to explain some features concerning the band structure. Figure 4 shows the diffuse reflectance spectra of as-prepared materials. The corresponding band gap values, obtained by the intersection point of the tangent of the absorption edge with extended line of the diffuse reflectance at lower wavelength, are 1.72 eV for Sb_2S_3 and 1.82 eV for Sb_2Se_3. The values of band gap coincide nearly with the reported data of 1.75 eV for Sb_2S_330 and 1.88 eV for Sb_2Se_3.[17b] The slight differences of band gap values in the products may be attributed to the high degree of crystallinity and great changes in the product sizes.

The two-point dc probe method of dark resistance measurement shows that the as-prepared single crystals have high dark resistance. The variation of R (Ω) with T (K) for bulk

(28) JCPDS Files No. 6-474 for Sb_2S_3; No. 15-861 for Sb_2Se_3.

(29) Wagner, C. D.; Riggs, W. W.; Davis, L. E.; Moulder, J. F.; Muilenberg, G. E. *Handbook of X-ray Photoelectron Spectroscopy*; Perkin-Elmer Corporation, Physical Electronics Division, Eden Prairie, MN: 1979.

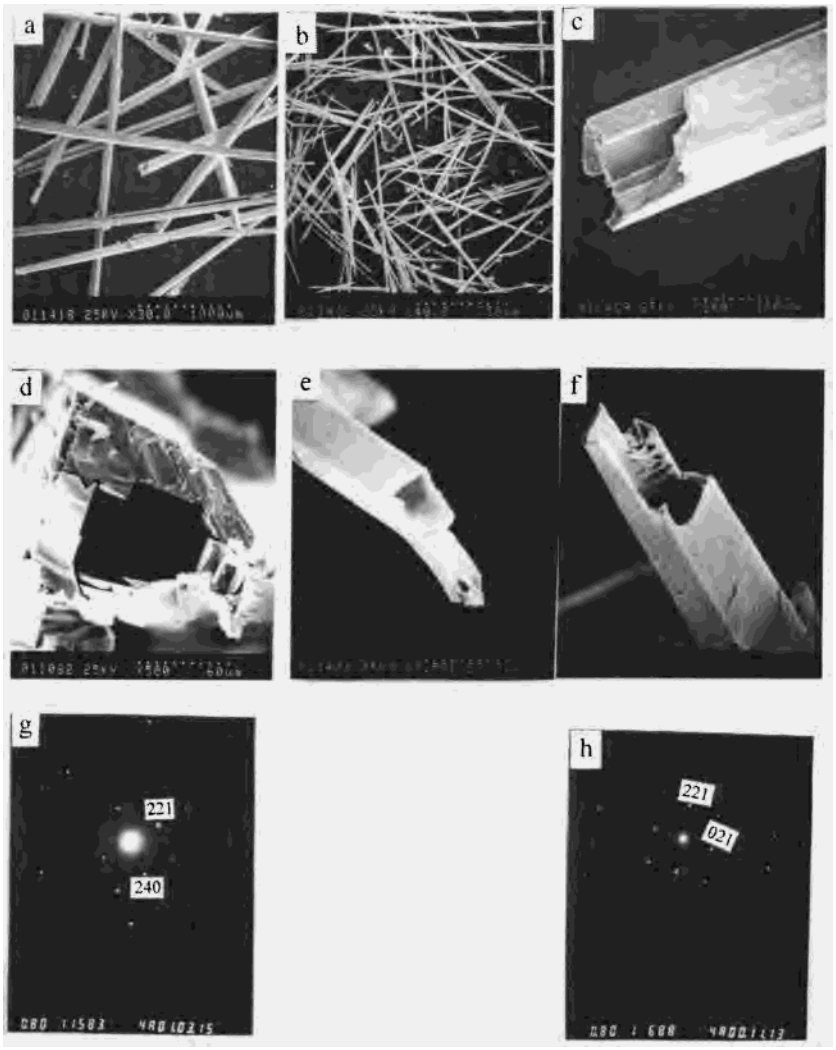

Figure 2. SEM images of Sb_2E_3 single crystals: (a) Sb_2S_3 and (b) Sb_2Se_3 bulk single crystals with low magnification; (c and d) Sb_2S_3 and (e and f) Sb_2Se_3 tubular single crystals with high magnification. ED pattern of (g) Sb_2S_3 and (h) Sb_2Se_3.

single crystals, depicted in Figure 5, indicates the semiconducting nature of the single crystals. The calculated resistivities of the single crystals are of the order of 10^5-10^6 Ω cm for Sb_2S_3 and 10^3-10^4 Ω cm for Sb_2Se_3, respectively. The values of resistivities are much lower than that of Sb_2E_3 (E = S, Se) reported in references.[17b,31] The low resistivity of the single crystals should be ascribed to the higher degree crystallinity, the smaller grain boundaries, and discontinuities in the as-prepared bulk single crystals.

In the whole solvothermal reaction process, to understand the possible mechanism of the formation of Sb_2E_3, controlled experiments under different conditions have been made. The detailed conditions and the results of the experiments are listed in Table 1, and all the products are characterized by XRD. The results of experiments 1−6 demonstrate that the optimal conditions for the growth of tubular crystals are that the temperature is not lower than 180 °C and the reaction time is not shorter than 7 days. In experiment 7, the formation of SbOCl derives from the traces of water in the absolute ethanol. Moreover, it is reported that the absolute ethanol would reduce the compound Sb_2O_3 to Sb at 360 °C.[32] Therefore, the formation of traces of Sb is reasonable in experiment 7 according to the contrast of the cell potential ($\varphi^0SbO^+/Sb = 0.21$ V > $\varphi^0Sb_2O_3/Sb = 0.15$ V). In light of the XRD results, the possible reaction steps and explanations for the formation of tubular crystals are as below:

$$SbCl_3 + H_2O \rightarrow SbOCl + HCl \quad (1)$$

$$SbOCl + CH_3CH_2OH \rightarrow Sb + CH_3CHO + HCl + H_2O \quad (2)$$

$$Sb + E\ (E = S, Se) \rightarrow (Sb_XE_Y)^{n-} \quad (3)$$

$$(Sb_XE_Y)^{n-} \xrightarrow{\text{self-assembly}} Sb_2E_3\ \text{(tubular crystals)} \quad (4)$$

Herein, the absolute ethanol plays a manifold role in the formation of tubular crystals. First, it can reduce the SbOCl to active atoms Sb, and the combination of trace active Sb with E to $(Sb_XE_Y)^{n-}$ in eq 3 will shift the chemical

(30) Yang, J.; Zeng, J. H.; Yu, S. H.; Li, Y.; Zhang, Y. H.; Qian, Y. T. *Chem. Mater.* **2000**, *12*, 2924.
(31) Rajpure, K. Y., Bhosale, C. H. *J. Phys. Chem. Solids* **2000**, *61*, 561.
(32) Chen, S. C. *the Important Inorganic Reaction* P170, Shanghai (Chinese), 1982.

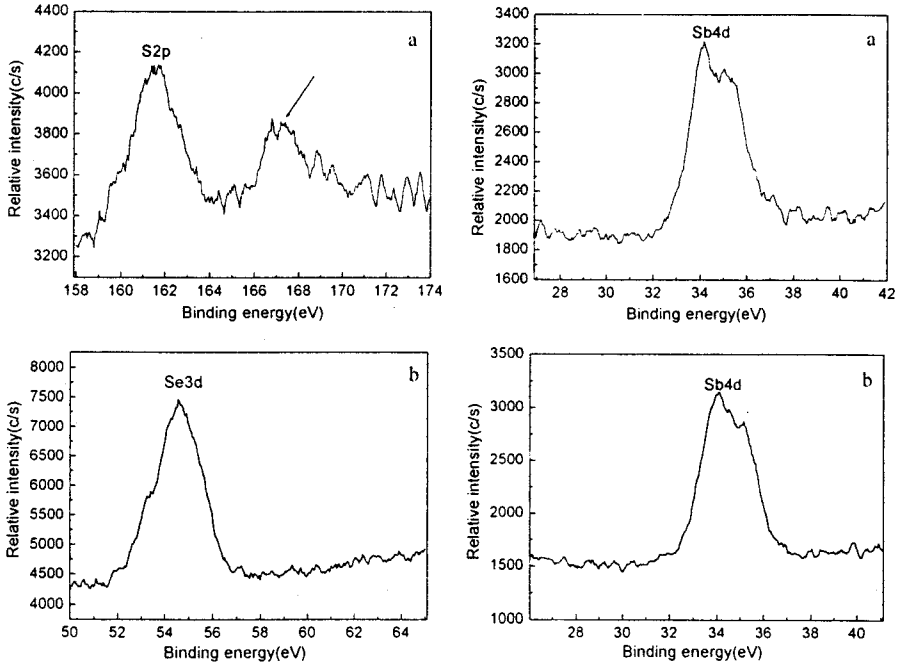

Figure 3. XPS spectra of (a) Sb_2S_3 (the arrowed peak indicates the S^{IV} peak) and (b) Sb_2Se_3.

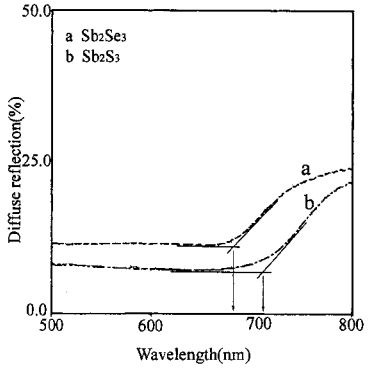

Figure 4. Diffuse reflectance spectra of the as-prepared single crystals.

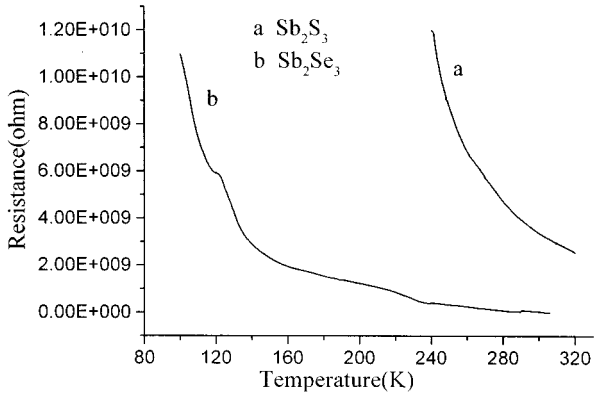

Figure 5. Variation of R (Ω) with T (K) for typical Sb_2E_3 bulk tubular single crystals.

equilibrium (eq 2) toward the right and lead to the complete reaction of SbO^+. The other important role of the absolute ethanol is its high solubility to the raw materials, which favors intimate mixing of the starting materials. In the solvothermal process, the diffusion control can be effectively removed by the use of the suitable solvent, which tends to afford an open crystalline structure. Sheldrick reported that

Table 1. Experimental Conditions and Results of the Experiments

no.	materials[a]	temp (°C)	time (days)	products	morphology
1	$SbCl_3$/S	150	7	Sb_2S_3	platelike single crystals
2	$SbCl_3$/S	150	4	Sb_2S_3	polycrystalline powders
3	$SbCl_3$/S	180	7	Sb_2S_3	acicular tubular single crystals[b]
4	$SbCl_3$/Se	180	2	Sb_2Se_3	nanorods
5	$SbCl_3$/Se	180	5	Sb_2Se_3	acicular tubular single crystals[c]
6	$SbCl_3$/Se	180	7	Sb_2Se_3	acicular tubular single crystals[b]
7	$SbCl_3$/ ethanol	180	7	SbOCl, Sb (trace)	
8	S/ethanol	180	7	S	
9	$SbCl_3$/Se	150	7	Sb_2Se_3, SbOCl, Se	
10	$SbCl_3$/S	180	7	Sb_2S_3	polycrystalline powders[d]
11	$SbCl_3$/Se	180	7	Sb_2Se_3	polycrystalline powders[d]

[a] The ratios of the $SbCl_3$ to E are 2:3. [b] The single crystals are well-defined and completely grown. [c] The single crystals are poorly completed. [d] The products are obtained without the relief of the solvent.

the solvent of methanol in the temperatures range 110−200 °C could greatly enhance solubility, diffusion, and crystallization but was still mild enough to leave molecular building blocks such as chains and rings intact to participate in the formation of polymeric anions.[23] Because of the similarity between ethanol and methanol in critical temperature (methanol 240.0 °C, ethanol 243.1 °C), viscosity (methanol 25 °C, 0.55 mPa·s, ethanol 25 °C, 1.06 mPa·s), and critical pressure (methanol 7.95 MPa, ethanol 6.38 MPa), we select the nontoxic ethanol as the solvent to control the diffusion and obtain the open crystalline structure.

The active atoms of Sb combine with E (E = S, Se) to form chain $(Sb_XE_Y)^{n-}$ units. As is well-known, the $(Sb_XE_Y)^{n-}$

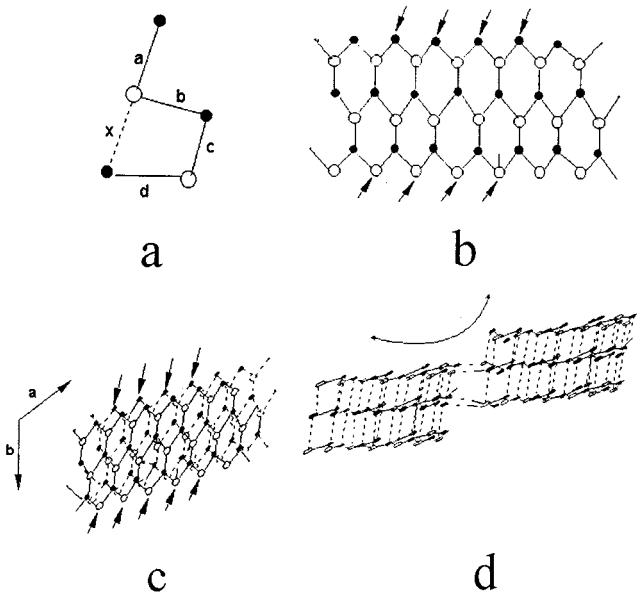

Figure 6. The schematic illustration of the formation of platelike and tubular single crystals for the products: (a) the structural units; (b) the Sb−S hexagonal layer structure; (c) view along [001] showing the linkage of two Sb−S hexagonal layers to form two-atom-thick sheets parallel to the (110) plane; (d) the linkage of two sheets (antimony, solid circles; chalcogen, open circles).

units are unusual chain structures, where Sb and E (E = S, Se) atoms are bound in infinite hexagonal sheets (Figure 6b), just like their predecessors of well-known carbon sheets. It is reported that the chalcogenides of antimony give rise to a variety of complex building units, including the $Sb_3S_6^{3-}$ semicube, which has been identified as a secondary building unit in Sb_2S_3[33] and a number of other templated antimony surfides;[19a] the flat s-shaped $[Sb_2S_2]^{2+}$, which are cross-linked (self-assembled) in two directions to form the $[Sb_3S_5]^-$ channels;[3] and the vertex-linked SbE_3^{3-} (E = S, Se) pyramidal species,[19a,23] from which a variety of chainlike structure motifs are derived. In the solvothermal process, the unusual chain structures play a crucial role in the growth of tubular crystals. The semicubic $[Sb_3S_6]^{3-}$ units serve to link together to form the two-dimensional sheets[34] paralleling to the [110] plane, in which each Sb atom and each S atom is bound to three atoms of the opposite kind. Besides the strong Sb−S interaction within the sheets, the existence of Sb−S bonds and van der Waals forces between two different sheets provides additional weaker secondary interaction[19a,34] to link double sheets and form two-atom-thick sheets (Figure 6c). These successive interactions would lead to the alignment of sequential sheets, which could result in the formation of platelike products when the reaction is terminated at a certain temperature. But at the edge of as-formed sheets, the existence of undersaturated dangling bonds of atom Sb or S (Figure 6b,c, arrowed) would induce the interaction of each other to eliminate the dangling bonds and reach the lowest energy level when the growth is terminated. The interaction of dangling bonds takes place either between two different sheets or within a sheet which leads to the rolling-up to form

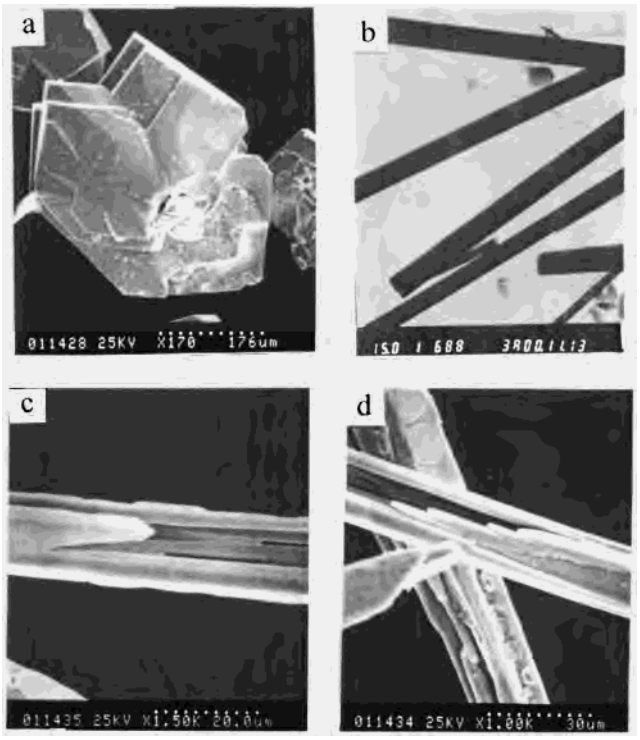

Figure 7. (a) SEM image of platelike bulk single crystals Sb_2S_3 obtained at 150 °C for 7 days, (b) TEM image of Sb_2Se_3 obtained at 180 °C for 2 days, and (c and d) SEM images of Sb_2Se_3 obtained at 180 °C for 5 days.

the circular structure, like carbon tubes.[11a] According to the SEM images (polygonal section tube), one can have the conjecture that the formation of a polygonal tube of Sb_2E_3 derives from the linkage of different sheets at certain angles by the Sb−S interactions (Figure 6d). These are quite different from the carbon tubes which derive from the rolling-up of the hexagonal carbon sheets, and show morphological similarity to WS_2 polygonal nanotubes,[11c] in which the two neighboring basal planes within a nanorod are usually located at ∼90° to each other.

To further study the proposed growth mechanism of the tubular crystals Sb_2E_3, the influence of temperature and reaction time on the morphology have been investigated in detail. It is found that the Sb_2S_3, obtained at 150 °C for 7 days, is hexagonal platelike single crystals (with dimensions of 180 × 200 μm, and a thickness of 50 μm, shown in Figure 7a), whereas the products, obtained at 180 °C for 7 days, are acicular tubular crystals (Figure 2c,d). Perhaps at the low temperature (150 °C), the driving force cannot make the layered-structure Sb_2E_3 to link together into tubules. As for Sb_2Se_3, it was composed of regular beltlike nanocrystals with diameter of about 200 nm and lengths up to several micrometers (Figure 7b) when the reaction lasted for 2 days at 180 °C. If the reaction time was prolonged to 5 days, all the regular beltlike nanocrystals transformed into poorly complete tubular crystals (Figure 7c,d). Meanwhile, at the edge of the tubular crystals just formed, some obvious patchlike bulges were observed, which indicated that the growth of tubular crystals was not complete. These necklike connections provide convictive proofs for the growth mechanism of tubular crystals, which is thought of as the linkage

(33) Bayliss, P.; Nowacki, W. Z. *Kristallogr.* **1972**, *135*, 308.
(34) Cotton, F. A.; Wilkinson, G. *Advanced Inorganic Chemistry*, 5th ed.; Wiley: New York; pp 404 and 504, 1988.

of two different sheets together to form the polygonal tubes. But when the reaction time was prolonged to 7 days, the well-defined and completely grown tubular crystals (Figure 2c,e,f) were obtained. All of the above results make one have the conjecture that the growth process of tubular crystals may be a self-assembly process, namely, the initial as-formed sheets (Figure 6b,c) may serve as an in situ source template and self-assemble together to form the secondary flakelike nanoparticles or beltlike nanocrystals. The adjacency of flakelike nanoparticles or beltlike nanocrystals offers more opportunities to self-assemble and forms the final platelike or acicular tubular single crystals with the prolongation of the reaction time. The suitable temperature and reaction time are more favorable for the self-assembly process and provide more possibility for the nucleation and growth of tubular crystals. However, we cannot obtain bulk tubular single crystals when we use the as-prepared nanorods or platelike single crystals as the raw materials under the same conditions (180 °C, 7 days). Perhaps the as-prepared raw materials have lost their activity.

Besides the influences of the temperature and reaction time on the final bulk tubular single crystals, it is also found that the solvent-relief process is important in the formation of the final products. In the case of the SRSS process, the gradual relief of the solvent in the form of gas from the autoclave results in the supersaturation of the solution, which can maintain the solution under the metastable condition during 7-day reaction time. The metastable condition is the key factor in the process of the growth of bulk single crystals. First, it could control the velocity of nucleation, which make the velocity of the nucleation and growth well-matched in the SRSS system. Second, it would lead to the formation of many crystal seeds. Subsequently, the crystal seeds grow into the secondary crystal seeds and the later crystal orientation growth. The contrast experiments show that the as-prepared products are flakelike nanoparticles or nanorods, obtained in the sealed autoclaves without the relief of the solvent (experiments 10 and 11).

Conclusion

A novel solvent-relief-self-seeding (SRSS) process has been successfully developed to synthesize Sb_2E_3 (E = S, Se) bulk polygonal acicular tubular crystals, using $SbCl_3$ and chalcogens (S, Se) as the raw materials in ethanol solution. In contrast, the normal solvothermal process only produced Sb_2E_3 (E = S, Se) polycrystalline powders. In the SRSS process, ethanol was very important for the synthesis of single crystals Sb_2E_3 (E = S, Se), which could reduce the SbO^+ ions into Sb atoms, and then the active Sb atoms recombined with elements E (E = S or Se) to Sb_2E_3. Details of the synthesis, characterization and analysis, resistivity, and spectroscopic characterization of the as-prepared bulk acicular single crystals were carefully investigated. Both the temperature and the reaction time have significant influence on the growth of bulk acicular tubular single crystals. The optimal reaction conditions were that the temperature was not lower than 180 °C and reaction time was not shorter than 7 days. The present SRSS process provides a practical low-temperature reaction pathway for the synthesis of other V−VI binary bulk single crystals. The as-prepared acicular tubular bulk single crystals can be used as containers or capsules for the host−guest chemistry to synthesize and tailor the structure of other materials.

Acknowledgment. Financial support from the Chinese National Foundation of Natural Sciences and Chinese Ministry of Education are gratefully acknowledged.

IC0107072